PROCEEDINGS OF SCIENCE

The Double Chooz Experiment

Luis Fernando Gomez Gonzalez[*†]
Universidade Estadual de Campinas - Unicamp, Campinas,SP, Brazil
APC, AstroParticule et Cosmologie, Université Paris Diderot, CNRS/IN2P3
E-mail: lfgomez@gmail.com

In this work we present the results of The Double Chooz Experiment in 227.93 live days with 33.71 GW-ton-years exposure using a 10.3 m^3 fiducial volume detector located at 1050 m from the reactor cores of the Chooz nuclear power plant in France. The experiment has observed 8,249 candidate electron antineutrino events while the expectation in case of θ_{13}= 0 was 8,937 events. From this deficit (rate analysis) plus spectral shape analysis we find $\sin^2 2\theta_{13} = 0.109 \pm 0.030(\text{stat}) \pm 0.025(\text{syst})$ witch exclude the no-oscillation hypothesis at 99.8% CL (2.9σ).

VIII International Workshop on the Dark Side of the Universe,
June 10-15, 2012
Rio de Janeiro, Brazil

[*]Speaker.
[†]on behalf of the Double Chooz Collaboration

PoS(DSU 2012)034

1. Introduction

The Double Chooz Experiment is one of the new generation reactor antineutrino disappearance experiments built to measure more precisely the mixing angle θ_{13}. For many years, the CHOOZ reactor neutrino experiment [1] had the best limit on the value of θ_{13}, but recently, the value of θ_{13}has been shown to be non-zero by the combination of results of KamLAND and solar [2, 3, 4], MINOS [5], T2K [6] and, more recently and precisely, by the new generation of reactor antineutrino disappearance experiments: Double Chooz [7], Daya Bay [8] and RENO [9]. Among the reactor experiments, the Double Chooz is the only one that uses the shape of the energy spectrum combined with the rate in the data analysis.

2. Detector

The Double Chooz Detector System consists of a main detector, witch comprises three different volumes, an outer veto and calibration devices (Figure 1). The three volumes main detector is made of four concentric cylindrical acrylic tanks which two volumes are filled with liquid scintillators and one with mineral oil. There is also a chimney in the center at the top. The innermost volume is filled with 10.3 m^3 of gadolinium loaded liquid scintillator and is called the ν-target (NT). The NT volume is surrounded by the γ-catcher (GC), a 55 cm thick cylindrical volume filled with Gd-free liquid scintillator, used to detect gamma rays that escaped from NT. Outside the γ-catcher there is the last inner detector volume called Buffer, a 105 cm thick cylinder filled with mineral oil. It work as a shield, absorbing the radioactivity of Photomultiplier Tubes (PMTs) and surrounding materials, as the mountains rocks.

Collecting the light generated in the NT and GC there are 390 PMTs, that will be described in section 2.2. The NT, CG, Buffer and PMTs constitute the main detector system, called the Inner Detector (ID). The next vessel outside the ID is a stainless steel cylinder optically separated from

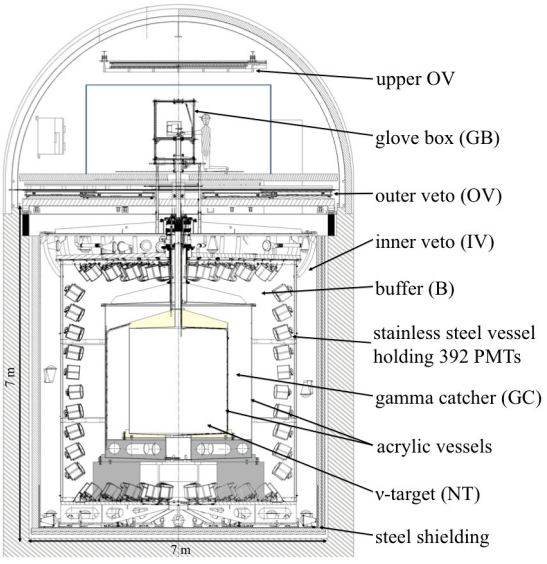

Figure 1: A cross-sectional view of the Double Chooz detector system.

the main detector. It is a 50 cm thick vessel filled with liquid scintillator and equipped with 78 8-inches PMTs. This volume is called Inner Veto (IV) and acts as cosmic muon veto and active shield. The whole detector is surrounded by 15 cm of demagnetized steel that function as a gamma ray shield. There is also a Outer Veto System covering the detector.

2.1 Double Chooz Liquids

The scintillator used in the NT was developed to fulfill the requirements of Gadolinium (Gd) solubility, optical transparency, radiopurity, chemical stability and chemical compatibility with the detector materials. The scintillator solvent chosen is an ortho-phenylxylylethane (o-PXE)/n-dodecane mixture at a volume ratio of 20/80 with a metalorganic complex of metal-β-diketone, $Gd(thd)_3$, Gd(III)-tris-(2,2,6,6-tetramethyl-heptane-3,5-dionate), to achieve the required Gd concentration. Furthermore, the wavelength shifters PPO (2,5-diphenyloxazole), as primary fluor, and bis-MSB (4-bis-(2-methylstyryl)benzene), as secondary, are added to shift the scintillation light into a more transparent region [10].
In Figure 2, we demonstrate the optical stability of the scintillator over about a year of data taking using the peak energy of neutrons captures on Gd. The energy response is stable within 1% during this period.

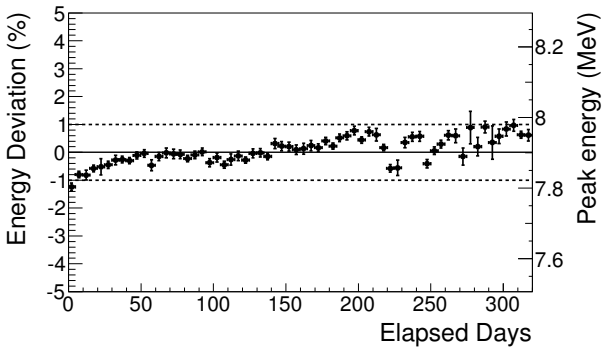

Figure 2: Average target detector response evolution in time, as measured by the mean energy of the Gd-capture peak arising from interaction of spallation neutrons in the NT.

A crucial parameter for the oscillation analysis is the absolute number of Hydrogen nuclei and its error. This error is minimized using well defined and pure chemicals and having a precise knowledge of the weights of each chemical added in the scintillator. The weight of NT scintillator was determined after thermalization with a precision of 0.04% and the hydrogen fraction is known with 0.3% relative precision.

2.2 Inner Detector PMTs

In the ID there are 390 10-inch Hamamatsu R7081 Photomultiplier Tubes (PMTs) [11] installed on the inner wall of the stainless steel buffer tank (submerged in the buffer paraffin oil) to collect light from the NT and GC. This PMT has a low background glass and each one is shielded by a mu-metal cylinder to suppress effects from the gamma shield and the earth's magnetic field [12]. Its base circuit is enclosed in a transparent epoxy resin and some are observed to generate light

flashes, causing false triggers. The high voltage of the 14 worst PMTs was turned off to reduce this false triggers. Nevertheless, this light flash signal is different from that of the neutrino signal and the false events can be identified and removed from the neutrino sample [13].

2.3 Inner Veto

The Inner Veto is an active shield, detecting muons crossing the detector (IV+ID) and screening the external radioactivity (gammas and spallation neutrons generated by muons in the surrounding material). It consists in a cylindrical stainless steel vessel (radius 3.3 m and height 6.8 m) optically separated from the ID with a 50 cm thick layer of liquid scintillator. All the IV surfaces are painted with a highly reflective white coating (AR100/CLX [14]) and the side walls of the buffer vessel are covered with reflective sheets (VM2000). The light produced in the IV is detected by 78 8-inch PMTs (Hamamatsu R 1408), divided into three parts: 24 PMTs in the top, 12 in the side walls at the mid way and 42 in the bottom. This PMTs were previously used in the IMB and Super-Kamiokande experiments and were modified for use in Double Chooz [15].

2.4 Electronics and Data Acquisition

The Double Chooz readout and data acquisition system for the ID and the IV detectors are shown in a Block diagram in Figure 3. The system consists in the High Voltage (HV) Supply (CAEN-A1535P [16]), the HV Splitter, the Front-End electronics (FEE), the Trigger system [17] and the flash-ADC digitizing electronics (CAEN-Vx1721) [18, 19], known as ν-fADC. The custom made HV Splitter is used to decouple the HV ($\sim$ 1.3 kV) and Signal (5 mV per PE) from the single PMT cable. After the decouple, the PMT signals are optimized (amplified, clipped, baseline restored and coherent noise filtered) by the FEE for digitization in the ν-fADC.

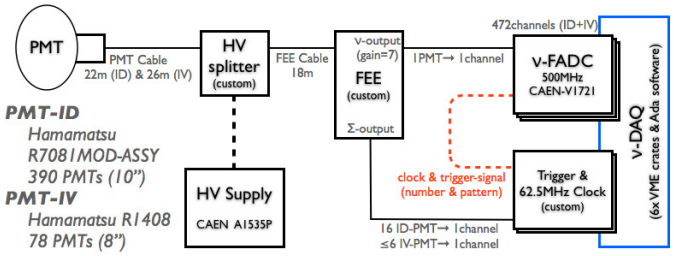

Figure 3: Block diagram of the Double Chooz readout and DAQ systems.

The detector is triggered by energy and multiplicity criteria at energies around 350 keV. Above 700 keV, the energy threshold used in data analysis, the trigger efficiency reaches 100% with negligible uncertainty. The IV triggers at $\sim$ 10 MeV which corresponds to 8 cm of a minimum ionizing muon track. The digitization of the signal is performed by the ν-FADC system witch consists on 64 CAEN-Vx1721(VME64x) [16] waveform digitizers with 8 channel per card. The fADC has 8-bit resolution at 500 MS/s. When the detector is triggered, a 256 ns waveform is recorded for each channel, containing $>$ 90% of the scintillation light emitted. Both ID and IV are readout using the same electronics upon any trigger of either the ID or IV.

3. Neutrino Analysis

The antineutrino candidate selection starts with the rejection of events with an energy below 0.5 MeV (where the trigger efficiency is not 100%), identified as light noise ($Q_{\max}/Q_{\text{tot}} > 0.09$ or $\text{rms}(t_{\text{start}}) > 40$ ns, where $Q_{\max}$ is the maximum charge collected by a single PMT, Q_{tot} is the total ID charge collected in a trigger and $\text{rms}(t_{\text{start}})$ is the standard deviation of the distribution of the first pulse start time on each PMT) [13] and any event within a 1 ms window following a tagged muon, to reduce correlated and cosmogenic backgrounds. This gives an effective veto time of 4.4% of the total run time. After this first rejection, the following 4 cuts are applied:

1. The time difference between consecutive triggers (prompt and delayed) must be in the interval: 2 μs $< \Delta$T $<$ 100 μs (where $\Delta T \equiv t_{\text{delayed}} - t_{\text{prompt}}$), as shown in Figure 4a. The lower cut is applied to reduce correlated backgrounds and the upper cut is approximately 30 μs capture time on Gd;

2. The prompt trigger must be in the interval: 0.7 MeV $< E_{\text{prompt}} <$ 12.2 MeV, as shown in Figure 4b;

3. The delayed trigger must be in the interval: 6.0 MeV $< E_{\text{delayed}} <$ 12.0 MeV (Figure 4b) and $Q_{\max}/Q_{\text{tot}} <$0.055;

4. Multiplicity cut: no additional triggers from 100 μs preceding the prompt signal to 400 μs after it, in order to reduce the correlated background.

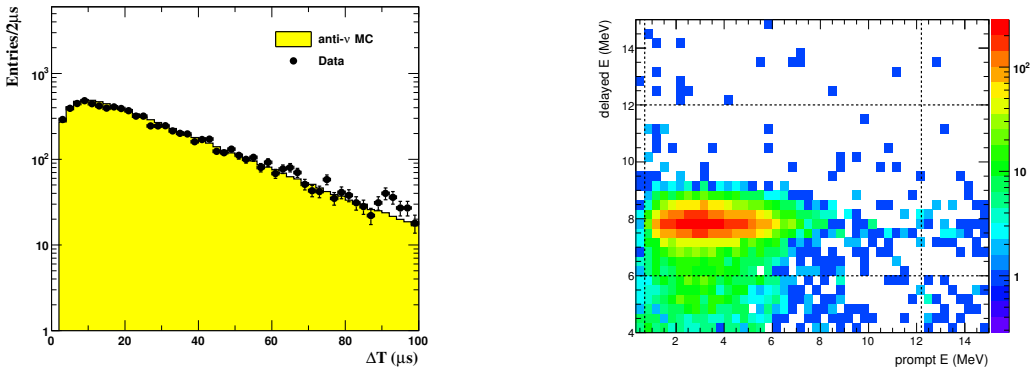

(a) Time difference between prompt and delayed triggers.

(b) Delayed energy versus prompt energy for time-correlated triggers.

Figure 4: Time and energy distribution of the neutrinos candidates.

After this selection a sample of 9021 candidate was found, and two additional cuts were applied:

1. No candidates within a 500 ms window after a high energy muon crossing the ID ($E_\mu >$ 600 MeV) to reduce cosmogenic isotopes events;

2. No candidates whose prompt signal is coincident with an OV trigger to reduce correlated background.

After the above two cuts a sample of 8249 candidates were found, equivalent to a rate of 36.2 $\pm$ 0.4 events/day.

4. Oscillation Results

To have a better separation of signal and background, the data is divided in two integration periods with different signal/background ratio. One set contains data periods where one reactor is operating at less than 20% of its nominal thermal power (according the data provided by EDF) and the other set contains all other data, typically when both reactors are running. This method adds information about background behavior to the fit: they have a different signal to noise ratio, but the background is constant during both periods. The distribution of Inverse Beta Decay (IBD) candidates in the two integration periods is described in Table 1.

	Reactors Both On	**One Reactor** $P_{th} < 20\%$	**Total**
Livetime [days]	139.27	88.66	227.93
IBD Candidates	6088	2161	8249
ν Reactor B1	2910.9	774.6	3685.5
ν Reactor B2	3422.4	1331.7	4754.1
Cosmogenic Isotope	174.1	110.8	284.9
Correlated FN & SM	93.3	59.4	152.7
Accidentals	36.4	23.1	59.5
Total Prediction	6637.1	2299.7	8936.8

Table 1: Summary of observed IBD candidates, with corresponding signal and background predictions for each integration period.

The IBD data is separated into 18 variably-sized bins between 0.7 and 12.2 MeV for each period for and the background populations were calculated based on the measured rates and the livetime of the detector during each integration period. The systematics and statistical uncertainties are propagated to the fit through a covariance matrix in order to properly account for correlations between energy bins [13]. With this data, a fit of the binned signal and background to a two-neutrino oscillation hypothesis was performed by minimizing a standard χ^2. The best-fit gives $\sin^2 2\theta_{13} = 0.109 \pm 0.030$ (stat.) ± 0.025 (syst) at $\Delta m^2_{31} = 2.32 \times 10^{-3}$ eV^2, with a $\chi^2/\text{NDF} = 42.1/35$ as shown in Figure 5. More information about how this analysis was performed and how the backgrounds were handled can be found in [13].

5. Conclusion

Double Chooz has observed 8,249 candidate electron antineutrino events and the expectation in case of θ_{13}= 0 is 8,937 events. From this deficit (rate analysis) plus spectral shape analysis we find $\sin^2 2\theta_{13}$ = 0.109 $\pm$ 0.030(stat) $\pm$ 0.025(syst) witch exclude the no-oscillation hypothesis at 99.8% CL (2.9σ). This is the first evidence for the θ_{13}value using the energy spectrum from

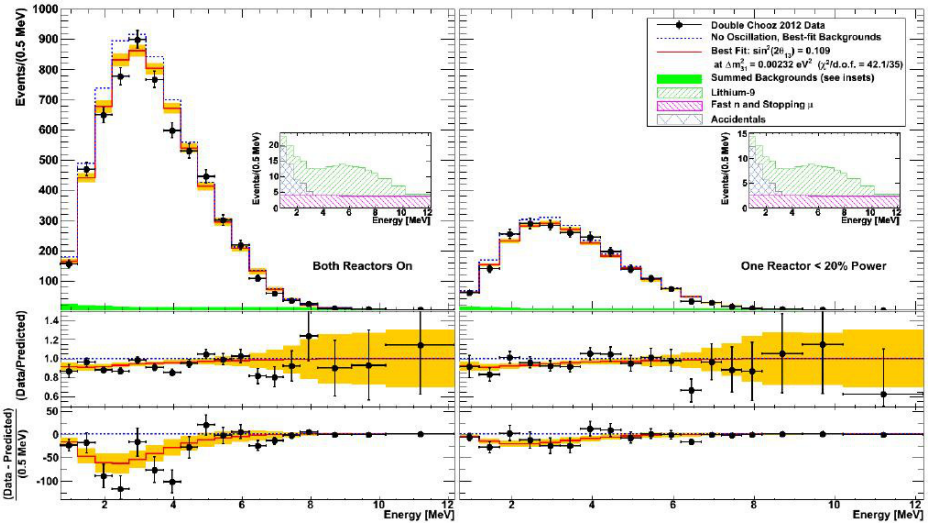

Figure 5: Measured prompt energy spectrum for each integration period (data points) superimposed on the expected prompt energy spectrum, including backgrounds (green region), for the no-oscillation (blue dotted curve) and best-fit (red solid curve) Inset: stacked spectra of backgrounds for both periods. Bottom: differences between data and no-oscillation prediction (data points), and differences between best fit prediction and no-oscillation prediction (red curve). The orange band represents the systematic uncertainties on the best-fit prediction.

reactor neutrinos, rather than simply their rate. This result is in excellent agreement with the results reported by Daya Bay [8], Reno [9], MINOS [5] and T2K [6] experiments as shown in Figure 6.

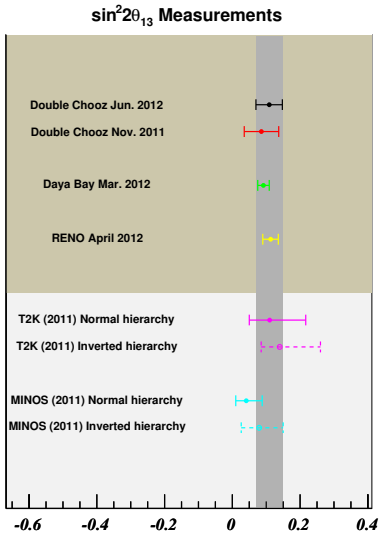

Figure 6: Comparison of the first Double Chooz publication [7], Daya Bay [8], RENO [9], T2K [6], and MINOS [5]. Error bars correspond to 1σ. For T2K and MINOS the CP phase δ has been arbitrarily fixed to $\delta = 0$.

We thank the French electricity company EDF, the European fund FEDER, the Région de Champagne Ardenne, the Département des Ardennes and the Communauté des Communes Rives de Meuse. We acknowledge the support of CEA and CNRS/IN2P3 in France, French LabEx UnivEarthS, Ministry of Education, Culture, Sports, Science and Technology of Japan (MEXT) and Japan Society for the Promotion of Science (JSPS), the Department of Energy and the National Science Foundation of the United States, the Ministerio de Ciencia e Innovación (MICINN) of Spain, the Max Planck Gesellschaft and the Deutsche Forschungsgemeinschaft DFG (SBH WI 2152), the Transregional Collaborative Research Center TR27, the Excellence Cluster "Origin and Structure of the Universe" and the Maier-Leibnitz-Laboratorium Garching, the Russian Academy of Science, the Kurchatov Institute and RFBR (the Russian Foundation for Basic Research), the Brazilian Ministry of Science, Technology and Innovation (MCTI), the Financiadora de Estudos e Projetos (FINEP), the Conselho Nacional de Desenvolvimento Científico e Tecnológico (CNPq), the Coordenação de Aperfeiçoamento de Pessoal de Nível Superior (CAPES), the São Paulo Research Foundation (FAPESP), the Brazilian Network for High Energy Physics (RENAFAE) in Brazil and the computer center CCIN2P3.

References

[1] M. Appolonio et al., Phys. Lett., B466, 415 (1999).

[2] G. L. Fogli, E. Lisi, A. Marrone, A. Palazzo and A. M. Rotunno, Phys. Rev. D84, 053007 (2011).

[3] The KamLAND Collaboration, Phys. Rev. D83, 052002 (2011).

[4] T. Schwetz et al., New J. Phys. 13, 109401 (2011).

[5] P. Adamson et al., Phys. Rev. Lett. 107, 181802 (2011).

[6] K. Abe et al., Phys. Rev. Lett. 107, 041801 (2011).

[7] Y. Abe et al., Phys. Rev. Lett. 108, 131801 (2012).

[8] F. P. An et al., Phys. Rev. Lett. 108, 171803 (2012).

[9] J. K. Ahn et al., Phys. Rev. Lett. 108, 191802 (2012).

[10] C. Aberle et al., JINST, 7, P06008 (2012).

[11] http://jp.hamamatsu.com/resources/products/etd /pdf/LARGE_AREA_PMT_TPMH1286E05.pdf.

[12] E. Calvo et al., Nucl. Instrum. Meth., A621, 222 (2010).

[13] Y. Abe et al., Phys. Rev. D 86, 052008 (2012).

[14] Max Perles et cie, http://www.maxperles.com/pdf /ftech_fr/ft_ar100clx_nov10.pdf (2012).

[15] K. Zbiri, arXiv:1104.4045 (2011).

[16] CAEN Corporation, http://www.caen.it/. The device was co-developed with APC.

[17] F. Beissel et al., “The Trigger and Timing System of the Double Chooz Experiment" (submitted to JINST).

[18] A. Cabrera, Nucl. Instrum. Meth. Phys. Res., Sect. A 617, 473 (2010).

[19] T. Akiri, Ph.D. thesis, Université Paris-Diderot, (2010).